RESEARCH PAPER

PCCP
www.rsc.org/pccp

Reactive scattering of Rydberg atoms: H* + D_2 → HD + D*†

Eckart Wrede,*[ab] Ludger Schnieder,‡[a] Karen Seekamp-Schnieder,‡[a] Britta Niederjohann[a] and Karl H. Welge§[a]

[a] *Faculty of Physics, University of Bielefeld, 33615 Bielefeld, Germany*
[b] *Department of Chemistry, University of Durham, Durham, UK DH1 3LE. E-mail: eckart.wrede@durham.ac.uk*

Received 16th November 2004, Accepted 23rd February 2005
First published as an Advance Article on the web 7th March 2005

The scattering of highly excited hydrogen Rydberg atoms, H*($n = 36$), with deuterium molecules in their rovibrational ground state, $D_2(v = 0, j = 0)$, has been investigated at a relative collision energy of 0.53 eV. Time-of-flight distributions of elastically/inelastically scattered H* Rydberg atoms and reactively scattered D* Rydberg atoms have been measured at different laboratory angles. The extracted rovibrationally resolved state distributions of the HD product molecules from reactive collisions resemble closely those reported for the corresponding ion–molecule reaction, $H^+ + D_2 \rightarrow HD + D^+$. This similarity is rationalised using the free electron model which predicts that the Rydberg electron acts as a spectator while the ionic reaction takes place.

I. Introduction

Reactions between Rydberg atoms and neutral molecules are a curious type of reaction between the usually studied 'extremes' of reactions between neutral atoms and molecules, and cations and molecules in their respective ground states. The binding energy of a highly excited Rydberg atom is very small (*e.g.* −0.9 meV for a hydrogen atom in $n = 40$). Thus, collisions involving a highly excited Rydberg atom are at least energetically very similar to the collisions involving the cation. The Bohr radius of the Rydberg electron in H*($n = 40$) is approximately 850 Å which is very large compared to the effective range of the interactions between the collision partners which is in the order of several ångströms. Furthermore, a Rydberg electron orbits the ion core relatively slowly compared to the relative velocities of the reactants in reaction dynamics experiments performed today, particularly if light reactants are involved: The classical, orbital speed of the electron in H*($n = 40$) is approximately 55 000 m s^{-1},[1] whereas the relative velocities in recent experiments of the H + D_2 reaction are of the order of 10 000 m s^{-1}.[2] Thus, the Rydberg electron does no longer move fast compared to the nuclear motion as assumed by the Born–Oppenheimer approximation. Obviously, reactions with Rydberg atoms do not follow the same dynamics as reactions involving ground state species.[1,3–5]

Matsuzawa describes collisions of highly excited Rydberg atoms with a neutral target molecule using the free electron model in which the interaction between the ion core and target is treated independently from the Rydberg electron-target interaction.[1] In the case where the latter interaction is unimportant, the scattering is dominated by the ion core-target interaction and the Rydberg electron acts as a spectator while the ion–molecule collision takes place.

Ref. 5 gives a good overview of the various experimental studies involving Rydberg atoms. In particular, Davies and coworkers have recently studied the inelastic scattering of Rydberg H* atoms (n = 30–50) with N_2 and O_2 molecules at 1.84 eV collision energy.[5] Their results confirm the free electron model and that the inelastic collisions of these systems resemble closely the corresponding ion–molecule scattering. They conclude that collisions between Rydberg atoms and non-polar molecules can be used to study ion–molecule collisions without the adverse influence of space charge effects usually encountered in ion beam experiments, particularly at low energies.

In this paper we present the first experimental study of the H* + D_2 → HD + D* Rydberg reaction. The remainder of this article is structured as follows: Section II describes the experimental set-up, the discovery and confirmation of the reactive scattering of Rydberg atoms. The experimental results are presented in Section III and discussed in Section IV. Conclusions follow in Section V.

II. Experiment

Experimental set-up

The experiments were carried out using the crossed molecular beams apparatus which was designed to measure the H + D_2 → HD + D ground state reaction and which is described in detail in ref. 2. A brief description is given here focussing on the elements which are relevant for this study. The schematic experimental set-up is shown in Fig. 1. A pure sample of *ortho*-D_2 was adiabatically cooled in a supersonic expansion from a liquid nitrogen cooled pulsed nozzle. In the resulting molecular beam, a population of D_2 molecules in their rovibrational ground state ($v = 0$, $j = 0$) of at least 97.5% was achieved. HI molecules in a second pulsed molecular beam, propagating parallel at a distance of 30 mm to the D_2 beam, were photodissociated using linearly polarised UV laser light of 266 nm wavelength. The direction of polarisation was chosen to direct the *slow* H atoms (with kinetic energy of 0.659 eV), corresponding to the formation of iodine atoms in their $^2P_{1/2}$ spin orbit excited state, towards the second molecular beam of D_2 molecules. In this configuration, the relative collision energy and its spread was determined as $E_{col} = 0.531 \pm 0.003$ eV.

The velocity distribution of the nascent atoms from elastic, inelastic or reactive collisions, *i.e.* H or D atoms, respectively, was measured using the Rydberg atom time-of-flight (TOF) technique.[6] The nascent atoms were excited into a high lying

† Presented at the Bunsen Discussion on Chemical Processes of Ions, Marburg, 15–17 September 2004.
‡ Permanent address: University of Tübingen, 72072 Tübingen, Germany.
§ Deceased 2001.

DOI: 10.1039/b417440b

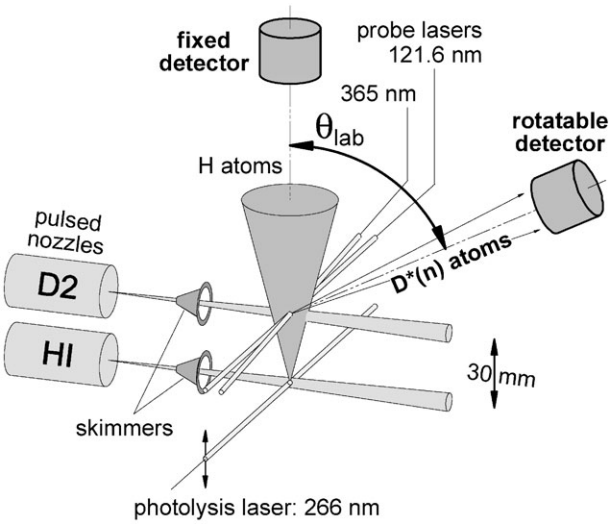

Fig. 1 Schematic set-up of the crossed beams experiment.

Rydberg state ($n \approx 35$) directly within the interaction volume by resonant two-photon excitation *via* the H/D(2p) state using two probe laser beams of 121.6 and 365.8 nm wavelength. The Rydberg-tagged atoms leave the interaction volume with their nascent velocity and are field ionised at the end of the drift region. The ions are subsequently detected by a secondary electron multiplier which can be rotated around the scattering centre in the plane defined by the H atom and D_2 molecular beams.

After the transformation of the TOF into the velocity or kinetic energy (both in the laboratory frame) of the detected atoms the centre-of-mass scattering angles, θ_{CM}, and internal energies of the nascent molecules, thus their quantum states, can be determined *via* energy and momentum conservation.

Elastic and inelastic scattering

The overall resolution of the experiment was optimised by means of measuring the TOF distribution of H atoms from elastic and inelastic collisions: $H + D_2(v = 0, j = 0) \rightarrow H + D_2(v', j')$. The probe lasers were tuned to the Lyman α and Rydberg transitions for H atoms. Fig. 2 shows the H atom lab kinetic energy spectrum (KES) recorded in this way at the laboratory scattering angle of $\theta_{lab} = 15°$. For high H atom lab kinetic energies, $E_{kin}(H) > 0.35$ eV, peaks corresponding to individual D_2 rotational levels of the vibrational ground state are clearly resolved. Note that the odd D_2 rotational levels were not populated because *ortho–para* transitions are forbidden in elastic/inelastic collisions. For energies lower than 0.35 eV, additional well resolved peaks appear only some of which can be attributed to rovibrationally excited $D_2(v' = 0–1, j')$ from inelastic collisions.

The inspection of the spectrum reveals that the unaccounted peaks seem to correspond to rotationally excited HD molecules formed in reactive collisions if one assumes that D atoms have been detected: $H + D_2(v = 0, j = 0) \rightarrow HD(v', j') + D$. These D atoms would have to reach the detector as Rydberg atoms, D*, because only Rydberg atoms with $n > 20$ were sufficiently excited to be field ionised by the detector field (~ 2000 V cm^{-1}). Furthermore, small electric fields (~ 10 V cm^{-1}) perpendicular to the drift path (one surrounding the scattering region and the other in front of the detector) ensured that ions were removed. This measure was necessary to eliminate signal created by the photoionisation of background gas with the high-energy laser radiation.

For comparison, the kinetic energy spectrum of D atoms from the 'ordinary' reaction, *i.e.* both probe lasers were tuned to D atom transitions to excite product D(1s) atoms into

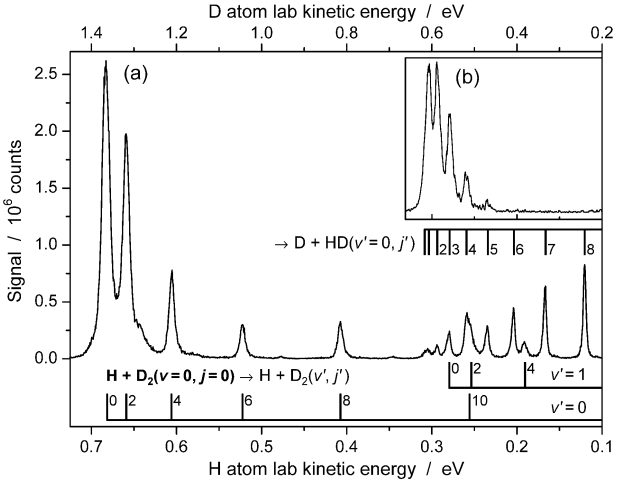

Fig. 2 (a) Kinetic energy spectrum of H atoms from elastic/inelastic collisions, $H + D_2(v = 0, j = 0) \rightarrow H + D_2(v', j')$, at a relative collision energy of $E_{col} = 0.53$ eV and a laboratory scattering angle of $\theta_{lab} = 15°$. Note that both probe lasers were tuned to H atom transitions to detect Rydberg H* atoms. The signal at low kinetic energies corresponds to detected Rydberg D* atoms, see text. (b) Kinetic energy spectrum of D atoms from reactive collisions, $H + D_2(v = 0, j = 0) \rightarrow HD(v', j') + D$ measured at the same collision energy and laboratory angle as in (a) with both probe lasers tuned to D atom transitions.

Rydberg D* atoms for detection, recorded at the same lab scattering angle is shown in the inset of Fig. 2. The peak positions are the same in both cases which confirms that the D* signal in the spectrum (Fig. 2, panel (a)) originates from reactive collisions. However, the rotational distributions are clearly distinct. While probing D atoms from the 'ordinary' reaction, the corresponding HD molecules show a cold rotational distribution.[2,7] In contrast, the D* atoms detected while probing *via* H atom transitions correspond to HD molecules with a nearly statistical rotational distribution (see later).

Scattering geometry

In order to explore the origin of the curious D* atom signal a more detailed discussion of the scattering geometry is necessary. Fig. 3 depicts a close-up of the interaction volume between the atomic and molecular beams. We will discuss the elastic/inelastic scattering of ground state H(1s) atoms and their detection first.

The H atoms expand from the photodissociation volume (overlap between HI molecular beam and photolysis laser) in a sphere-shaped shell the thickness of which is given by the diameter of the photolysis laser. Note that the pulse length of this H atom shell is only ~90 ns (FWHM) which is negligible compared to the pulse length of 140 μs for the D_2 beam. The

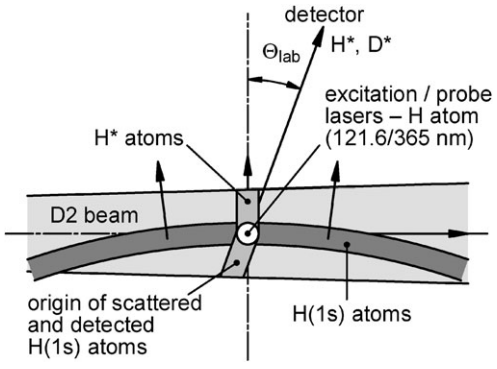

Fig. 3 Schematic geometry of the scattering region. The drawing is approximately to scale: thickness of expanding H atom shell 1 mm, D_2 beam diameter 4 mm (FWHM), probe laser diameter 1 mm.

shell of H atoms sweeps through the D_2 molecular beam and collisions occur in the entire interaction volume. In order to be detected, a scattered H atom has to (i) fly into the probe volume (overlap between both probe lasers), (ii) be excited into a Rydberg state when the probe lasers are fired and (iii) have the right direction of travel towards the detector. This means that nascent H atoms have to be 'born' within the area labelled ''origin of scattered and detected H(1s) atoms'' in Fig. 3 which includes the probe volume.

However, if the incident H atom shell crosses the probe lasers as they are fired, a short, intense Rydberg H* atom beam is created, which is still travelling through the D_2 molecular beam. Thus, collisions between H* atom and D_2 molecules can occur which may have the following outcomes:

$$H^* + D_2(v = 0, j = 0) \rightarrow H^* + D_2(v', j') \quad (1)$$

$$\rightarrow HD(v', j') + D^* \quad (2)$$

In the following sections we will refer to these processes as an elastic/inelastic or non-reactive Rydberg scattering (1) and reactive Rydberg scattering or Rydberg reaction (2).

In the latter case, reactive scattering occurs and the Rydberg electron is transferred from the reactant H* atom to the product D* atom.

III. Results

Test measurements

The mechanism proposed in the previous section can easily be tested by changing the positions of the probe laser beams.

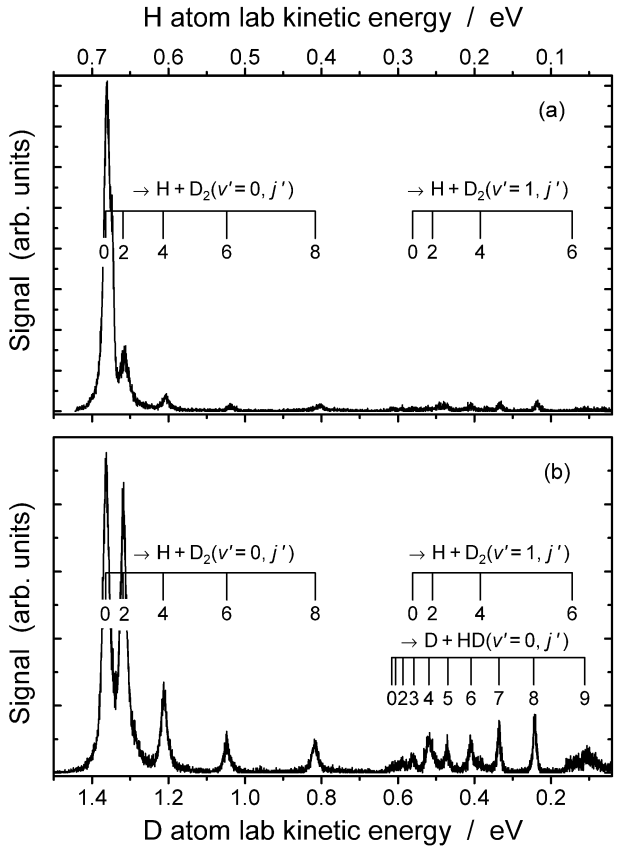

Fig. 4 Kinetic energy spectra of detected H*/D* Rydberg atoms using different probe laser beam geometries. Collision energy $E_{col} = 0.53$ eV, laboratory scattering angle $\theta_{lab} = 15°$. Both probe lasers were tuned to H atom transitions. (a) Probe volume 3 mm above the centre of the D_2 beam: H(1s) atoms are exited into a Rydberg state *after* elastic/inelastic scattering has occurred. (b) Probe/excitation volume 3 mm below the D_2 beam: H atoms are excited into a Rydberg state *before* the collision, *i.e.* H* atoms collide with D_2 molecules.

Fig. 4 shows kinetic energy spectra recorded with both probe lasers aligned above and below the D_2 molecular beam. The VUV probe laser was tuned to the H atom Lyman α transition. In order to further discriminate between H and D atoms the Rydberg excitation was tuned to the H(2p) → H(n = 36) transition at 27 334.8 cm^{-1} which lies between the D(2p) → D(n = 34 and 35) transitions at 27 332.0 and 27 337.3 cm^{-1}, respectively. Care was taken not to saturate the elastic peak corresponding to $D_2(v' = 0, j' = 0)$ molecules. The timing between the photolysis and probe lasers was optimised to give maximum H* atom signal at $\theta_{lab} = 0°$.

If the probe lasers are situated above the D_2 beam then no Rydberg excitation can occur before any H(1s) + D_2 collisions take place and only ground state H(1s) atoms from elastic/inelastic collisions will be excited into Rydberg states and subsequently detected. It is evident from Fig. 4(a) that the D* signal from Rydberg reactions is greatly reduced. Some D* signal remained because the probe lasers could only be moved by ±3 mm with respect to the centre of the D_2 beam which had a diameter of 4 mm (FWHM) at the centre of the interaction region.

The second spectrum, shown in Fig. 4(b), was recorded with the probe lasers placed 3 mm below the centre of the D_2 beam. The D* signal is increased dramatically which is consistent with the proposed reaction of H* Rydberg atoms with D_2 molecules, eqn. (2). Fig. 4(b) shows also that the inelastic H* signal increases with respect to the elastic H* signal. This dramatic change in the rotational distributions of the D_2 and HD nascent molecules leads to the conclusion that the scattering of Rydberg H* atoms with D_2 molecules proceeds *via* different mechanisms compared to the corresponding ground state collisions, H(1s) + D_2.

As a further test, an experiment with the complementary isotopic variant, D + H_2, was conducted using the trace amounts of DI in our HI sample as D atom precursor (the gas supply system had been used with deuterated species for different experiments). A pure sample of *para*-H_2 was used for the H_2 molecular beam. Both probe lasers were tuned to D atom transitions and aligned at the centre of the H_2 beam. The relative collision energy for the D + H_2 collisions was E_{col} = 0.31 eV and one spectrum was recorded at a laboratory scattering angle of $\theta_{lab} = 11°$ which is shown in Fig. 5. As predicted, H* signal from Rydberg reactions, $D^* + H_2(v = 0, j = 0) \rightarrow HD(v' = 0, j') + H^*$, is present in the spectrum. Because of their lighter mass, the H* atoms are now recorded at shorter times-of-flight than the D* atoms and thus appear at

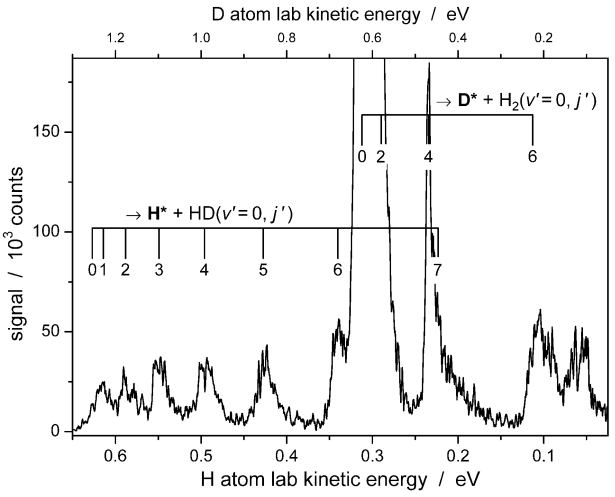

Fig. 5 Kinetic energy spectrum of scattered H*/D* atoms from D* + $H_2(v = 0, j = 0)$ collisions at a relative collision energy of $E_{col} = 0.31$ eV and a laboratory scattering angle of $\theta_{lab} = 11°$. Both probe lasers were tuned to D atom transitions.

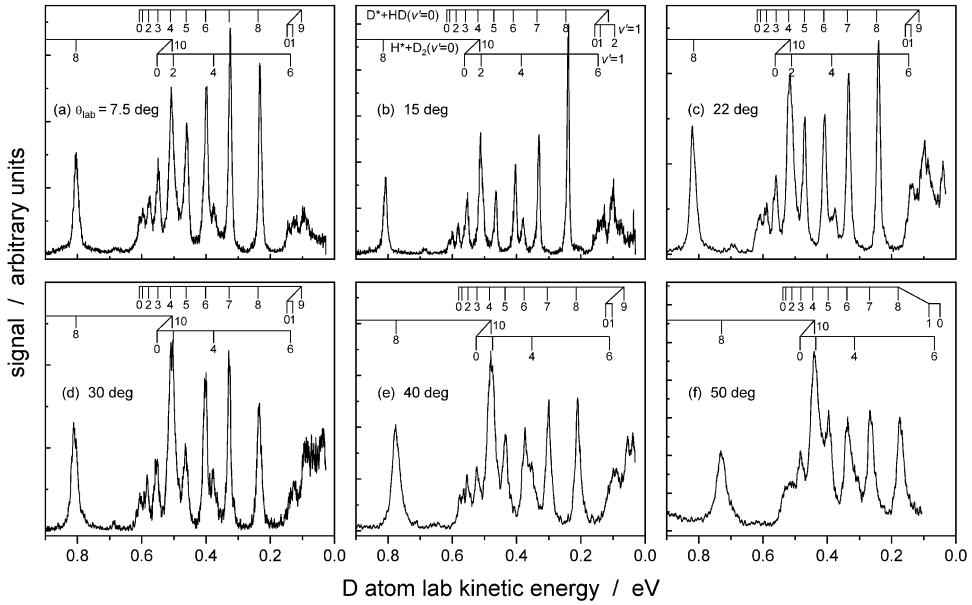

Fig. 6 Kinetic energy spectra of scattered H*/D* atoms from H* + $D_2(v = 0, j = 0)$ collisions at different lab scattering angles, θ_{lab}, and a collision energy of $E_{col} = 0.53$ eV. Both probe lasers were tuned to H atom transitions.

higher kinetic energies in Fig. 5 as the TOF spectrum is converted into the KES assuming the same mass for all detected particles.

Kinetic energy spectra

Kinetic energy spectra from H* + D_2 Rydberg collisions were recorded at six lab scattering angles in the range of $\theta_{lab} = 7.5$–50°. As before, the probe lasers were tuned to H atom transitions and, for reasons of experimental simplicity, aligned at the centre of the D_2 beam. Fig. 6 depicts the low energy part of each spectrum which contains the D* signal from Rydberg reactions. The H* signal corresponding to H* + $D_2(v' = 0, j' = 8)$ is included for comparison. The peaks corresponding to individual rovibrational levels of the HD product molecules are well resolved although some occasional overlap with H* signal from non-reactive collisions occurs.

The rotational distributions of the product HD($v' = 0$, j') molecules, as seen in Fig. 6, appear to be roughly statistical particularly for small lab scattering angles, $\theta_{lab} \leq 22°$, and for low product rotational states. To investigate this further, relative final state populations of the HD molecules, $P(v', j')$, were extracted from the KES measured at $\theta_{lab} = 7.5$ and 15°. A sum of Gaussian–Lorentzian profiles centred at each peak position, including the H* peaks from non-reactive scattering, was fitted to the KES. The relative populations are then given by the area of each fitted peak with respect to the total area associated with D* signal from Rydberg reactions. The relative rotational HD populations are superimposed on the fitted KES in Fig. 7 together with the statistical prior distribution[8] for HD($v' = 0$) products. The comparison between the measured and the prior distributions, which do not account for any angular momentum constrains, indicates that the HD product states are mainly statistically populated, however, some pronounced deviations from the prior distribution are evident. The higher rotational levels, $j' = 7$ and 8, show significantly higher populations than predicted by this simple statistical model, particularly in the spectrum recorded at $\theta_{lab} = 15°$. In order to quantify this behaviour fully state-resolved differential cross sections in the centre-of-mass system would need to be extracted. Unfortunately, due to the limited quality and scale of the current data set (see next section) this must await future studies.

Total angular distribution

The angular distribution of the total D* signal is an important input for the determination of differential cross sections (DCS).[2] TOF spectra were accumulated for 1000 or 3000 laser shots over the accessible range of lab scattering angles from 7.5 to 143°. The lab angle was changed in a pseudo-random pattern between the individual acquisitions to prevent long term drifts from influencing the data. The total signal corresponding to D* atoms was extracted from the individual spectra, although, due to overlapping peaks the total D* count rate from Rydberg reactions may be slightly contaminated by some H* signal. Fig. 8 shows the angular dependence of the

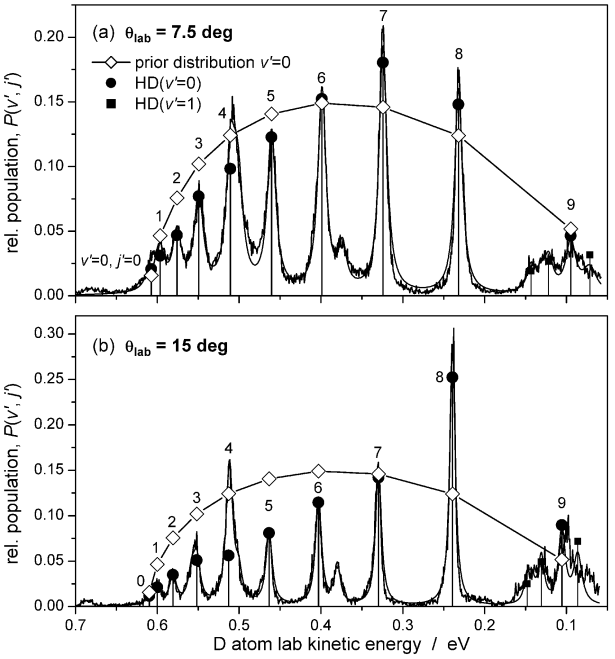

Fig. 7 Relative rotational populations of HD product molecules from H* + $D_2(v = 0, j = 0)$ reactions extracted from fits to the KES recorded at two different lab scattering angles, θ_{lab}. The fit curve (smooth) is superimposed on the measured KES. The populations correspond to the fitted area of each peak. The statistical prior distribution for HD($v' = 0$, j') is superimposed for comparison.

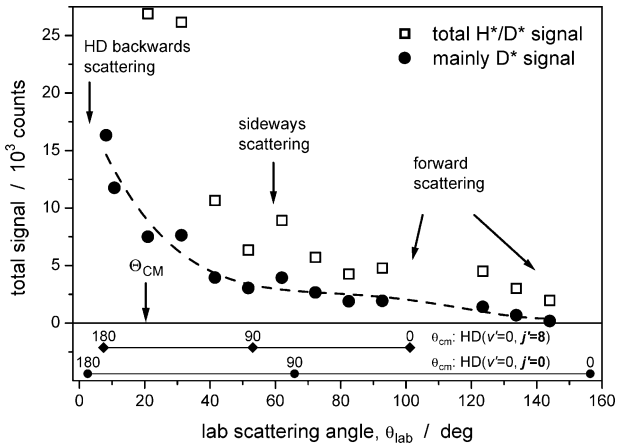

Fig. 8 Total H* and D* signal from $H^* + D_2(v = 0, j = 0)$ collisions as a function of laboratory scattering angle, θ_{lab}. Total H*/D* signal (open squares), total D* signal from Rydberg reactions (filled circles) extracted from the low energy part of the collected spectra (see text). The dashed line provides a guide for the eye to the D* signal. The correspondence between D* laboratory angles and product HD centre-of-mass scattering angles is depicted in the lower panel for fast ($j' = 0$) and slow ($j' = 8$) products. Θ_{CM} indicates the laboratory angle of the centre-of-mass motion.

combined H*/D* and the extracted D* signal. The large scatter of the data between neighbouring angles gives an indication of the experimental error of this measurement. As alluded to earlier, the quality of this data set is insufficient to extract DCS. However, the laboratory angular distribution of the products already provides some information about the shape of the DCS. The lab scattering angles for backwards ($\theta_{cm} = 180°$), sideways (90°) and forwards (0°) scattered HD products are indicated in Fig. 8. The shape of the total angular distribution suggests that the HD products from Rydberg reactions are mainly backwards scattered. Although, the measured signal at larger lab angles could be reduced due to secondary scattering of the nascent Rydberg atoms as they pass through the D_2 molecular beam, in particular at lab angles near 90°. Yet, the KES spectra recorded at $\theta_{lab} = 50°$ does not show any broadening of the peaks which could be attributed to secondary scattering.

IV. Discussion

Equivalence between Rydberg and ionic scattering

Where comparison was possible, the results resemble very much those for the corresponding ionic reaction, $H^+ + D_2 \rightarrow HD + D^+$. Gerlich has reported measurements of the ionic reaction at 0.5 eV collision energy and a laboratory scattering angle of 5°, the spectrum of which shows partial resolution of HD product rotations.[9] The rotational distribution is very similar to the one recorded in this study at $\theta_{lab} = 7.5°$ (Fig. 7(a)).

This similarity is consistent with the free electron model described in the introduction. Thus, the Rydberg electron can be viewed as a spectator while the ionic $H^+ + D_2$ collision takes place. After the collision, the Rydberg electron will attach itself to the nascent ion core which provides the positive charge centre. During the entire collision process the positive charge of the ionic reactant, the ionic transition state and the ionic product will still be shielded by the Rydberg electron such that the colliding system appears neutral to the outside 'world'. Therefore, this kind of scattering between Rydberg atoms and neutral molecules offers an ingenious way to study the corresponding ionic reactions in a neutral experimental environment without the adverse influence of space charge effects present in ion beam experiments.

The reported total reaction cross sections at $E_{col} = 0.53$ eV for the neutral ground state and ionic reactions are 0.27 $Å^2$ and ~ 10 $Å^2$, respectively.[7,10] The experimental count rates of detected D* atoms from the Rydberg reaction were estimated to be at least 20 times higher than those for D atoms from the ground state reaction under otherwise similar experimental conditions. The relative signal strengths are again consistent with the proposed mechanism that Rydberg scattering is equivalent to the corresponding ionic collisions.

In principle, a second reactive channel could be present: $H^* + D_2 \rightarrow HD^* + D$ corresponding to the $H^+ + D_2 \rightarrow HD^+ + D$ ion–molecule reaction. This channel could not be observed as the endothermicity of this reaction is 1.87 eV,[11] which exceeds even the total energy of 0.72 eV for these experiments.

Comparison with results from ionic reactions

To the best of our knowledge, no rovibrationally resolved DCS for the ionic $H^+ + D_2 \rightarrow HD + D^+$ reaction have been reported to date. The only comparable study by Gerlich using an ion beam approach has already been mentioned above.[9] Other angle and (partially) state resolved ion beam studies of $H^+ + H_2$ collisions and their isotopic variants were conducted at far higher collision energies.[12–15] Krenos and co-workers have investigated $H^+ + H_2$ collisions in various isotopic forms at collision energies between 1 and 7 eV.[11] Experimental, state unresolved DCS were compared to theoretical ones calculated using the trajectory surface hopping method. They conclude that the ionic reaction proceeds *via* a short-lived H_3^+ intermediate and that backwards scattering dominates for collision energies below 3 eV.

Further theoretical investigations of the unimolecular dissociation of the H_3^+ complex using semiclassical and quantum methods have been reported.[16–18] In particular, Brass and Schlier have carried out classical trajectory calculations to study the formation, the relaxation of the internal degrees of freedom and the break-up of the H_3^+ collision complex at low collision energies in the range from 0.1 to 1.5 eV.[18] They demonstrated that the internal vibrational motions relax on a time scale comparable to the average rotational period and lifetime of the complex. This means that the lifetime is long enough to allow the internal motions to be distributed statistically whereas the correlation between the break-up direction and the initial collision axis is not lost. The authors conclude that the traditional criterion of forward–backward symmetric scattering is not necessarily a good indicator for complex formation and should be applied with caution.

The experimental results for the $H^* + D_2$ Rydberg reaction reported here are in good qualitative agreement with the results by Krenos *et al.*[11] and by Brass and Schlier,[15] in particular. The nearly statistical HD product distribution confirms the complex formation. The measured angular distribution, which indicates that the HD molecular product is mainly scattered in the backwards direction, implies that the lifetime of the complex is short compared to its rotational period. This agreement reinforces the equivalence between Rydberg and ionic reactions.

Differences between Rydberg and ionic collisions

Clearly, due to the presence of the Rydberg electron, collisions with Rydberg atoms are different from ionic reactions. Because of the minuscule binding energy of the Rydberg electron, *e.g.* just 10 meV for $H^*(n = 36)$, ionising collisions (such as Penning, associative, dissociative or collisional ionisation) can easily occur.[3] Furthermore, the Rydberg electron can be captured by the neutral reactant molecule in attaching collisions (electron transfer) with the atomic cation and the molecular anion as products. However, these ionising and attaching collision could not be observed in the experiments reported here as all ions were removed from the flight path to the detector by small electric fields.

Obviously, in cases where the free electron model is violated the analogy between Rydberg atom and ion–molecule collisions no longer holds. Very large cross sections for collisions involving polar molecules have been reported.[3] Here, due to the huge dipole moment of the Rydberg electron, the dipole–dipole forces can lead to interaction distances in the order of the radius of Rydberg orbit.

Relevant for the current study are n or l changing collisions where the Rydberg state changes between the reactant and nascent Rydberg atoms.[3] As described in the experimental section, the Rydberg state of the H* atom was chosen not to coincide energetically with a Rydberg state of the product D* atom. Thus, the Rydberg state had to change during the reaction. However, the energy difference between the H*(n = 36) Rydberg state and the nearest D* energy levels, $n' = 34$ and 35, is just 0.4 meV. The corresponding change of the kinetic energy release is too small to be observed in the KES. Furthermore, no evidence for higher n changing collisions is apparent from the data.

The rotational period of the HD_2^+ complex is 1.2 ps (assuming the D_{3h} equilibrium geometry with bond lengths of 0.873 Å, ref. 19) which becomes comparable to the orbital period of the Rydberg electron in particular for intermediate Rydberg states (*e.g.* 7 ps for $n = 36$ and 1.2 ps for $n = 20$, ref. 1). Thus, for certain combinations, the orbit of Rydberg electron could be in resonance with the rotation of the collision complex. This may lead to increased collisional ionisation or enhanced population of particular product quantum states. The large deviations from the prior distribution for some HD product states (Fig. 7) could be associated with these resonances. However, far more detailed experimental and theoretical studies are necessary to clarify this hypothesis.

In principle, the range of the Coulomb field of the H^+ ion core can be controlled *via* the size of the orbit of the Rydberg electron, *i.e.* *via* the initial H* Rydberg state. Matsuzawa predicts that the cross section will only depend weakly on the initial n quantum number of the H* atom within the spectator model for the Rydberg electron.[1] However, for lower n the spectator model for the Rydberg reaction will eventually break down and significant deviations from the ionic scattering should be observed in the cross sections.

V. Conclusions

The experiments reported in this study demonstrate that the reaction between highly excited hydrogen Rydberg atoms and deuterium molecules is very similar to the corresponding ionic reaction, $H^+ + D_2 \rightarrow HD + D^+$. This finding is consistent with free electron model in which the ion–molecule interaction dominates and the Rydberg electron acts as a spectator while the ion–molecule reaction takes place. This type of reaction offers a new and ingenious way to measure the dynamics of ionic reactions in a neutral experimental environment and with unprecedented resolution compared to ion beam studies.

For the $H^* + D_2(v = 0, j = 0) \rightarrow HD(v', j') + D^*$ Rydberg reaction, rovibrationally resolved product state distributions have been measured at different laboratory scattering angles. The limited scope and quality of the current data does not yet allow the extraction of state-to-state differential cross sections for this reaction. However, future experiments are underway which should provide high-quality data to boost theoretical studies in this field. Current theoretical treatments of the $H^+ + H_2$ reaction and its isotopomers employ quasi-classical surface hopping, approximate quantum-classical and restricted quantum methods.[20–22] The quality of these predictions have still to be evaluated against sufficiently detailed experiments.

Rydberg reactions are important and interesting in their own right. In particular, the possibility of resonances between the orbit of the Rydberg electron and the rotation of the collision complex may lead to interferences in the cross sections for these reactions.

Metastable Rydberg species have been reported in laser ablation plasmas[23,24] the chemistry of which is only poorly understood in detail. In general, one can expect that long-lived Rydberg atoms are created *via* ion–electron recombination in plasmas, particularly in their outer, cooler regions and their presence will influence the plasma chemistry.

Acknowledgements

The work was financed by the German Science foundation (grant SCH 435/3). EW thanks the participants of the 85th International Bunsen Discussion Meeting *Chemical Processes of Ions – Transport and Reactivity*, Marburg, Germany, September 15th–17th 2004, for many helpful and encouraging discussions.

We dedicate this article to our colleague, supervisor and friend Professor Karl Heinz Welge (deceased 2001).

References

1 M. Matsuzawa, in *Rydberg States of Atoms and Molecules*, ed. R. F. Stebbings and F. B. Dunning, Cambridge University Press, Cambridge, 1983, pp. 267–314.
2 L. Schnieder, K. Seekamp-Rahn, E. Wrede and K. H. Welge, *J. Chem. Phys.*, 1997, **107**, 6175.
3 F. B. Dunning and R. F. Stebbings, in *Rydberg States of Atoms and Molecules*, ed. R. F. Stebbings and F. B. Dunning, Cambridge University Press, 1983, pp. 315–353.
4 T. F. Gallagher, *Rydberg Atoms*, Cambridge University Press, Cambridge, 1994.
5 B. R. Strazisar, C. Lin and H. F. Davis, *Phys. Rev. Lett.*, 2001, **86**, 3997.
6 L. Schnieder, W. Meier, K. H. Welge, M. N. R. Ashfold and C. M. Western, *J. Chem. Phys.*, 1990, **92**, 7027.
7 L. Bañares, F. J. Aoiz, V. J. Herrero, M. J. D'Mello, B. Niederjohann, K. Seekamp-Rahn, E. Wrede and L. Schnieder, *J. Chem. Phys.*, 1998, **108**, 6160.
8 R. D. Levine and R. B. Bernstein, *Molecular Reaction Dynamics and Chemical Reactivity*, Oxford University Press, Oxford, 1987.
9 (*a*) D. Gerlich, *Ber. Bunsen-Ges. Phys. Chem.*, 1982, **86**, 471; (*b*) D. Gerlich, PhD thesis, University of Freiburg, Germany, 1977.
10 J. G. Wang and P. C. Stancil, *Phys. Scr., T*, 2002, **96**, 72.
11 J. R. Krenos, R. K. Preston, R. Wolfgang and J. C. Tully, *J. Chem. Phys.*, 1973, **60**, 1634.
12 H. Udseth, C. F. Giese and W. R. Gentry, *Phys. Rev. A*, 1973, **8**, 2483.
13 K. Rudolph and J. P. Toennies, *J. Chem. Phys.*, 1976, **65**, 4483.
14 V. Hermann, H. Schmidt and F. Linder, *J. Phys. B*, 1978, **11**, 493.
15 G. Niedner, M. Noll, J. P Toennies and C. Schlier, *J. Chem. Phys.*, 1987, **87**, 2685.
16 E. Pollak and C. Schlier, *Acc. Chem. Res.*, 1989, **22**, 223.
17 M. Berblinger, C. Schlier, J. Tennyson and S. Miller, *J. Chem. Phys.*, 1992, **96**, 6842.
18 O. Brass and C. Schlier, *J. Chem. Soc., Faraday Trans.*, 1993, **89**, 1533.
19 W. Cencek, J. Rychlewski, R. Jaquet and W. Kutzelnigg, *J. Chem. Phys.*, 1998, **108**, 2831.
20 C. Schlier, U. Nowotny and E. Teloy, *J. Chem. Phys.*, 1987, **111**, 401.
21 M. Chajia and R. D. Levine, *Phys. Chem. Chem. Phys.*, 1999, **1**, 1205.
22 H. Kamisaka, W. Bian, K. Nobusada and H. Nakamura, *J. Chem. Phys.*, 2002, **116**, 654.
23 F. Claeyssens, R. J. Lade, K. N. Rosser and M. N. R. Ashfold, *J. Appl. Phys.*, 2001, **89**, 697.
24 R. E. Leuchter, *Appl. Surf. Sci.*, 1998, **127**, 626.

